Catalysis Today 176 (2011) 103–109

Contents lists available at ScienceDirect

Catalysis Today

journal homepage: www.elsevier.com/locate/cattod

Improved oxygen storage capacity on CeO_2/zeolite hybrid catalysts. Application to VOCs catalytic combustion

I. Maupin*, J. Mijoin, J. Barbier Jr., N. Bion, T. Belin, P. Magnoux

Université de Poitiers, Laboratoire de Catalyse en Chimie Organique, UMR CNRS 6503, 40 avenue du Recteur Pineau, 86022 Poitiers Cedex, France

ARTICLE INFO

Article history:
Received 29 September 2010
Received in revised form 2 February 2011
Accepted 4 February 2011
Available online 8 March 2011

Keywords:
Basic zeolites
Ceria
Oxygen storage capacity
Isotopic exchange
Catalytic oxidation
VOCs

ABSTRACT

The aim of this work was to evaluate the possible synergy in hybrid catalysts composed of the two types of solids and to study their performances in the catalytic combustion of isopropanol.

Several catalysts, based on cerium oxide and zeolites, for the catalytic oxidation of volatile organic compounds (VOCs), especially isopropanol, were tested. This study was assessed by determining the catalysts activity, selectivity and deactivation at various temperatures after 5 h of reaction. An important part of the work was the preparation and characterization of the catalysts, in particular the study of oxygen storage and mobility. Hybrid catalysts exhibit a synergy effect in terms of oxygen storage capacity and oxygen isotopic exchange. However, even if a synergy effect is also observed in catalytic oxidation over some samples, the oxygen mobility does not ensure better results in isopropanol combustion.

1. Introduction

The volatile organic compounds (VOCs) are well known atmospheric pollutants. Governmental regulation qualifies the VOCs as compounds which, except methane (CH_4), carbon oxides and carbonates, contain carbon and hydrogen. Both chemical elements can be replaced by other atoms such as halogen, oxygen, sulfur, nitrogen or phosphorus. These compounds are in gas phase under normal conditions of temperature and pressure. A European guideline project completes this definition by adding that each organic product with vapor pressure superior to 10 Pa under normal conditions of temperature and total pressure is a VOC. In the USA, the limit vapor pressure chosen is equal to 0.13 Pa [1].

VOCs also have a toxic effect on human health, as the main part is carcinogenic, mutagenic and/or harmful for human reproduction and development [1]. Furthermore, their presence in the atmosphere can cause chemical reactions supporting the formation and the accumulation of noxious compounds, or ozone [1].

For several years, this environmental and health problem has been one of the main preoccupations in developed countries. Many conventions have tried to heighten public awareness of it and find appropriate solutions. The Geneva Convention, signed in November 1991, aims at limiting VOC emissions [1]. According to the nature and the concentration of the pollutants, thermal incineration, catalytic oxidation, condensation, absorption, adsorption or recovery by trapping and storage using membranes or biological systems are some of the used techniques, which present advantages and drawbacks [1,2].

Catalytic oxidation is an interesting alternative because of the low energy cost and the relatively low temperatures needed in comparison with thermal combustion, which limit the formation of noxious oxides [2].

In literature several catalysts, like pure metal oxides [3–8], more especially alumina promoted or not with noble metals or oxides, were tested [9–20]. Among potential catalysts, ceria (CeO_2) proved to be effective because of its oxygen storage capabilities [21]. Some mixtures between ceria and oxides and/or noble metals were also studied [22,23]. Several works were performed over zeolites doped or not with metals [24–35]. Basic zeolites and particularly faujasite ones showed also interesting properties for VOCs combustion [36–40].

Moreover, faujasite zeolites are characterized by the presence of one type of large cages (supercages), 13 Å in diameter and ball-shaped, accessible through a 12-ring window with a free aperture of 7.4 Å, which is larger than the size of most of the organic molecules.

In a catalytic combustion point of view, the major issue is the difficulty to anticipate chemical reactions (condensation, polymerization, etc.) during the oxidation. Catalytic tests were performed over isopropanol, which can be partially transformed into acetone and/or propene. Various works were published explaining the mechanism of acetone production, like the one proposed by Chanda and Mukherjee [41] using copper catalysts. They proved that the

* Corresponding author. Tel.: +33 5 49 45 39 14; fax: +33 5 49 45 37 79.
E-mail address: irene.maupin@univ-poitiers.fr (I. Maupin).

0920-5861/$ – see front matter © 2011 Elsevier B.V. All rights reserved.
doi:10.1016/j.cattod.2011.02.003

oxidation of isopropanol is complex because of the isopropanol trend to be dehydrated into propene.

The aim of our work is the development of the best catalyst for the total oxidation of VOC (isopropanol) in carbon dioxide (CO_2). The mixture of ceria, which presents interesting performances in VOCs catalytic oxidation, and faujasite (NaX), which exhibits a particular porosity with supercages, would allow the containment of the molecules next to the active sites. Exchange or oxide clusters incorporation are also expected. In addition, the enhancement of oxygen exchange between gas and solid phase (catalyst) and/or oxygen storage capacity would allow better VOCs combustion. Consequently, the main part of this work was the ceria and faujasite mixture preparation to obtain hybrid catalysts with high oxygen storage capacity, especially in dynamic conditions, and with ability for oxygen exchange. Samples were then tested to check this particular preparation profit in catalytic experiments.

2. Experimental

2.1. Catalysts preparation

Cerium dioxide (CeO_2) was prepared by calcining $Ce(NO_3)_3{\cdot}6H_2O$ (Fluka, purity > 99.0%) under air flow (200 mL/min) with a heating rate of 1 °C/min from room temperature to 110 °C with a hold of 1 h. Then the samples were heated up to 550 °C (2 °C/min) overnight.

Faujasite zeolites were supplied by Axens (Si/Al = 1.2).

Several hybrid catalysts were synthesized by mixing ceria and NaX faujasite in various weight proportions (20, 35, 50, 65 and 80 wt% ceria, respectively named HT20, HT35, HT50, HT65 and HT80). The preparation began by a mechanical mixture of the two solids. Thereafter the samples were pelletized under pressure (1.5 t/cm^2) and sieved (between 0.2 and 0.4 mm) to ensure intimate mixture. Finally, the sieved mixtures underwent a high temperature treatment under air flow up to 600 °C. Other samples were prepared to complete the study: C20 (20.7 wt% ceria) which was not pelletized and not sieved before high temperature treatment and M50 which is a simple mechanical mixture between ceria and faujasite (50 wt% ceria) without any high temperature treatment.

2.2. Catalyst characterization

2.2.1. Acidic properties

The catalysts acidity was characterized by pyridine adsorption followed by FTIR spectroscopy. The catalyst was compacted (3 t/cm^2) into a pellet of 16 mm diameter and 2 cm^2 surface. The activation was carried out under air flow equal to 60 mL/min during 12 h at 450 °C (2 °C/min). After cooling until 400 °C, the cell was kept for 1 h under a secondary vacuum (10^{-5} mbar). Pyridine injection was performed for 5 min at 150 °C after pressure stabilization at 2 mbar. The total elimination of physisorbed pyridine was obtained after a treatment at 150 °C for 1 h under secondary vacuum. The thermodesorption of pyridine was then carried out at four temperatures (150, 250, 350 and 450 °C) and the IR spectra were recorded at room temperature. IR spectra were recorded in a Nexus Nicolet spectrometer equipped with DTGS detector (Deuterium TriGlyceride Sulfur) and KBr beam splitter, with a resolution of 2 cm^{-1} and 64 scans. The adsorption of pyridine results in the appearance of two adsorption bands corresponding to pyridium ion, PyH^+ (1545 cm^{-1}), and pyridine bonded to Lewis acid sites, PyL (1450 cm^{-1}). Brønsted and Lewis acid sites were determined and quantified by the subtraction between P_∞ (spectrum of the catalyst before adsorption of pyridine) and P_{150} (spectrum of the catalyst after adsorption and desorption of pyridine at 150 °C). The extinction coefficients of PyH^+ and PyL bands, i.e., respectively 1.13 and 1.28 cm/μmol, were taken from a previous study [42].

2.2.2. Textural properties

Adsorption–desorption isotherms of nitrogen at −196 °C were carried out with a Micromeritics ASAP 2010 apparatus. The sample was kept under vacuum at 90 °C for 1 h and then at 350 °C for 3 h. Micropore volumes were obtained by the *t*-plot method and the Dubinin–Radushkevich equation was used to calculate the mesoporosity.

2.2.3. Structural properties

XRD characterizations (λ_{Cu} = 1.542 Å, 10° 2θ to 75° 2θ, 0.02° 2θ and 4 s by step) were also performed to check the structures of the several synthesized hybrid catalysts. The space group of ceria is *Fm*3*m* and the one of faujasite is *Fd*-3*m*. These two compounds present a cubic structure, face centered cubic for the ceria. XRD patterns were recorded over a Brüker D5005 diffractometer thanks to Diffrac+ software (XRD Wizard and XRD Commander) and interpreted with Eva and Topas softwares. Scherrer method was used to calculate the particle sizes of ceria and NaX for all the samples. The formula is the following one: $D = (K \times \lambda)/(\mathrm{FWMH} \times \cos\theta)$ in which D is the particle size, K a numerical constant equal to 0.9, λ the wavelength of the incident X-rays, FWMH the width at half weight of the peak and θ the incident or Bragg angle [43].

2.2.4. Oxygen storage capacities (OSCC–OSC)

The oxygen storage capacity was measured following the oxidation of carbon monoxide in transitory regime without oxygen in gas phase by mean of two different techniques (OSC and OSCC). The amount of available oxygen in the catalyst is given by the amount of carbon dioxide formed during the reaction: $CO(g) + 1/2\ O_2(s) \rightarrow CO_2(g) + \square(s)$. The oxygen storage capacities of the samples were measured at 400 °C using a conventional set-up described in a previous report [44]. The sample (30 mg for NaX and 5 mg for the other catalysts) was first brought to 400 °C under flowing He (30 mL/min) before pretreatment under O_2. To calculate the total amount of available oxygen in the sample (OSCC), pulses of CO (0.267 mL) were injected every 2 min up to a maximum sample reduction. Such a treatment gives information about both surface and bulk mobile oxygen species. However, in a catalytic point of view surface species are often more involved under dynamic conditions. Therefore, OSC experiments were also carried out by re-oxidizing the samples with O_2 pulses. Then, alternating pulses of CO and O_2 were injected to probe the amount of O_2 (average of three alternations) immediately available in these materials, which is supposed to be mainly involved in the catalytic process. Results were obtained thanks to a gas phase chromatograph equipped with a TCD and a Porapak Q type column (i.d. = 1/4 in., L = 0.5 m) and oxygen storage capacities (OSCC and OSC) are expressed in $\mu mol_{CO_2}/g$ from the CO_2 formation (after CO pulses), which corresponds to the number of oxygen atoms ($\mu mol_O/g$) removed from the solid.

2.2.5. $^{18}O_2/^{16}O_2$ isotopic exchange experiments

Oxygen isotopic exchange experiments were carried out in a closed-loop reactor system. A recirculating pump was used in order to avoid any diffusion and mass transport effects in the gas phase that affect partial pressures of different isotopomers measured by mass spectrometry (Pfeiffer vacuum). Experimental set-up and data treatment were described in more detail in previous papers [45,46]. Prior the isotopic oxygen exchange experiments, the samples were heated up to 580 °C during 1 h (10 °C/min) under $^{16}O_2$ flow (D_{O_2} = 50 mL/min). Thereafter, the sample was evacuated for 15 min and the temperature was brought to the desired temperature for the isotopic exchange study. We carried out temperature-programmed isotopic exchange (TPIE) from 280

Table 1
Main physico-chemical properties of catalysts.

	Specific surface area (m^2/g)	External surface area (m^2/g)	Pore volume (cm^3/g)	Micropore volume (cm^3/g)	Mesopore volume (cm^3/g)	Average pore size (Å)	nL (a.u.)
NaX	761.7	6.0	0.31	0.30	0.01	16.5	7.76
HT20	619.7	25.0	0.30	0.26	0.04	33.4	
C20	605.8	13.5	0.28	0.24	0.03	37.8	7.78
HT35	532.4	38.0	0.28	0.22	0.06	34.2	8.50
HT50	423.3	46.4	0.25	0.17	0.08	33.9	
M50	348.4	54.5	0.25	0.14	0.11	35.5	4.72
HT65	267.9	57.6	0.22	0.11	0.11	36.7	
HT80	206.7	55.5	0.20	0.08	0.11	37.1	2.92
CeO_2	83.6	80.6	0.21	0.03	0.18	41.0	0.44

to 580 °C (2 °C/min) to determine the temperature range for which the different samples exchange oxygen. Then we performed same kind of experiments in isotherm conditions named isotherm isotopic exchange (IIE) at 450 and 550 °C. From the partial pressures evolution of the different isotopomers of the gas phase, i.e. $^{18}O_2$, $^{16}O^{18}O$ and $^{16}O_2$ (respectively P_{36}, P_{34} and P_{32}), we calculated the number of exchanged atoms for each sample studied thanks to a Pfeiffer mass spectrometer and the Quadstar 32-Bit Dispsav software.

2.3. Catalytic experiments

The gaseous feed used for catalytic combustion was composed of 1360 ppm of isopropanol in synthetic and wet air (80% nitrogen, 20% oxygen, 33% relative humidity, 1.2 mol% water). Transfer lines were heated at 120 °C to avoid condensation. The VOC destruction was carried out in a fixed bed reactor (i.d. = 5 mm, length = 90 cm) at atmospheric pressure and followed as a function of time (for 5 h) at constant temperature. Catalyst samples (catalyst mass = 0.14 g, catalyst height = 1.2 cm) were supported on a small plug of glass wool in a vertical glass tubular reactor. The reactor was inserted into an oven and temperature was measured by a thermocouple inserted near the catalyst bed. The gas hour space velocity (GHSV) was kept constant in all experiments (18,000 h^{-1}, calculated at room temperature and pressure).

The used catalysts were previously activated overnight under air flow at 450 °C in the same reactor.

The experimental setup was coupled with a gas chromatograph (Varian 3400) equipped with two columns: a packed column (Porapak Q) with a thermal conductivity detector (TCD) to analyze air and carbon dioxide and a capillary one (30 m VF-5 ms with 0.25 mm of internal diameter and 0.25 μm film thickness) with a flame ionization detector (FID) to observe hydrocarbons, i.e. isopropanol and secondary products of reaction (basically acetone and propene).

After reaction, catalysts were recovered and the carbon content of these samples was measured by total burning at 1020 °C under helium and oxygen with a CEinstruments NA2100 Protein analyzer.

3. Results and discussion

3.1. Characterization

The textural properties in terms of specific surface area, pore volume and average pore size are summarized in Table 1. Except for the average pore size, the evolution of these results seems to follow a continuous and logical trend. Indeed the specific surface area, the external surface, the pore, micropore and mesopore volumes tie in with the expected values according to the relative amounts of each compound. Fig. 1a shows the sameness between interpolated values (calculating the weighted sum by the mass of each compound) and experimental results of HTs preparations about the specific surface area, which increases with the faujasite amount. According to Table 1, such an observation was also made for the two other kinds of preparations, simple mechanical mixture (M50) and simple high temperature treatment (C20), and for other results obtained that are pore, micropore and mesopore volumes (not plotted here). Therefore, since the pore and micropore volumes are close to the expected volumes, it could be assumed that ceria does not plug the zeolite pores. Ceria would rather be located on the external surface or on pore mouth. Moreover, thermal treatment of the catalysts (whether it corresponds to high temperature treatment for HTs and C20 samples or to pretreatment before N_2 sorption analysis) does not seem to significantly redisperse ceria since the specific surface area is not enhanced. However, the presence of ceria, even in low amount on the faujasite, seems to enhance the average pore size, near the one of pure ceria (Fig. 1b). A morphological variation or a structural modification of ceria could explain this phenomenon and could be due to the high temperature treatment for C20 and for HTs preparations and to N_2-physisorption pretreatment for M50. For HT50 and M50, the only difference is the high temperature treatment. The decrease of the external surface from M50 to HT50 could be explained by a sintering of ceria particles and/or a collapsing of zeolite structure. However, the specific surface area and the micropore volume are enhanced by high temperature treatment, which seems to invalidate the second hypothesis. Therefore, a morphological rearrangement of CeO_2 particles on the zeolite surface creating micropores appears to be more probable.

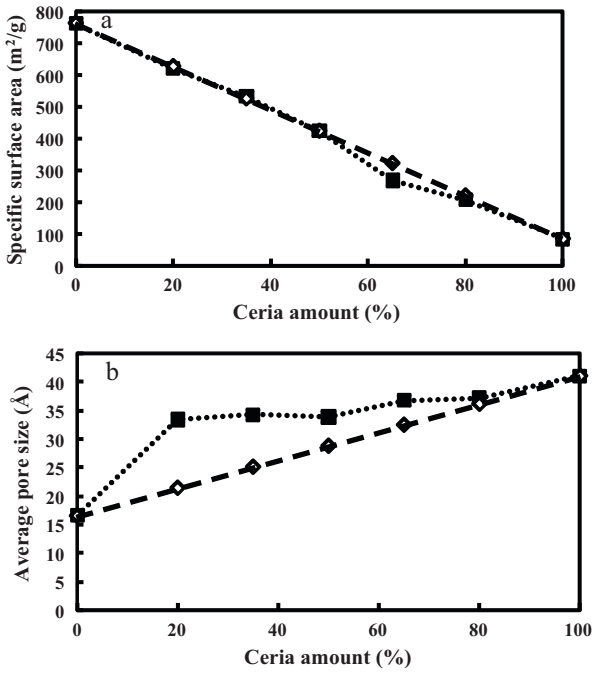

Fig. 1. Comparison between interpolated values (◊)(· · · · · ·) and experimental results (■) (—) for specific surface area (a) and average pore size (b) of HTs catalysts.

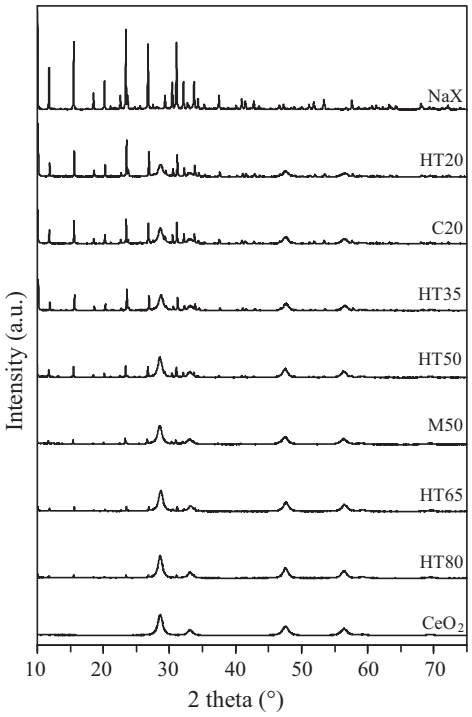

Fig. 2. X-ray diffraction patterns of the CeO_2/NaX (x:1 − x) catalysts.

Table 1 also presents the results of adsorption of pyridine followed by IR spectroscopy. Neither ceria nor faujasite exhibit Brønsted acid sites and consequently hybrid catalysts do not either. The number of Lewis acid sites (nL) able to retain pyridine at 150 °C is expressed in arbitrary unit. Indeed, the band due to real Lewis acid site and the band due to the coordination between pyridine and the zeolite compensation cation (Na^+) are mingled. Nevertheless, even if the extinction coefficient corresponding to the Py–Na^+ interaction was not yet determined a relative comparison is possible according to the weighted sum by the mass of each compound. The results show an improvement of the "Lewis acidity" (with a maximum for HT35) on hybrid catalysts.

Moreover, the crystallographic structure of each compound does not seem to be affected by the hybrid catalysts preparation or thermal treatment since significant peaks of ceria and NaX are visible in each XRD spectrum (Fig. 2). The average particle sizes are equal to 13 nm and 104 nm for respectively ceria and faujasite (with weak difference between each hybrid catalyst). Consequently, most of the ceria is not able to enter the pores of faujasite (about 7 Å) and may stay on the external surface of the zeolite.

3.2. Study of the oxygen mobility

Surface mobility phenomena play an important role in catalysis [47]. Oxygen mobility on oxide solids as well as on supported metal catalysts has been largely studied by using the oxygen isotopic exchange technique [46,47]. Nevertheless, it is often difficult to distinguish between surface and bulk oxygen mobility for oxides with high oxygen mobility [48]. Generally, temperature-programmed isotopic exchange (TPIE) gives information about the general behavior of the bare catalyst while the isothermal isotopic exchange (IIE) estimates the kinetic parameters of the surface mobility [49]. Three mechanisms of isotopic exchange of oxygen on oxides on supported metal catalysts can be observed: the homoexchange or equilibration (type I) without the participation of oxygen from the solid catalyst (Eq. (1)), the simple heteroexchange (type II) with the participation of only one oxygen atom from the solid

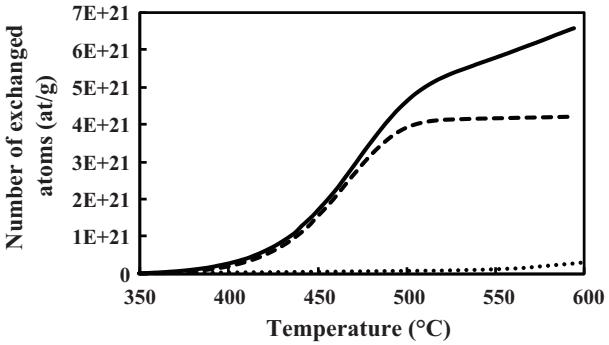

Fig. 3. Determination of the total quantity of oxygen atoms exchanged by temperature-programmed isotopic exchange over ceria (- - -), NaX (· · · · · ·) and C20 (—).

(Eqs. (2) and (3)) and the multiple heteroexchange (type III) with the participation of two oxygen atoms from the solid (Eqs. (4)–(6)) [46,47,50]:

$$^{18}O_2(g) + {}^{16}O_2(g) \rightarrow 2\,{}^{18}O{}^{16}O(g) \quad (1)$$

$$^{18}O_2(g) + {}^{16}O(s) \rightarrow {}^{18}O{}^{16}O(g) + {}^{18}O(s) \quad (2)$$

$$^{18}O{}^{16}O(g) + {}^{16}O(s) \rightarrow {}^{16}O_2(g) + {}^{18}O(s) \quad (3)$$

$$^{18}O_2(g) + 2\,{}^{16}O(s) \rightarrow {}^{16}O_2(g) + 2\,{}^{18}O(s) \quad (4)$$

$$^{18}O{}^{16}O(g) + 2\,{}^{16}O(s) \rightarrow {}^{16}O_2(g) + {}^{16}O(s) + {}^{18}O(s) \quad (5)$$

$$^{18}O{}^{16}O(g) + 2\,{}^{18}O(s) \rightarrow {}^{18}O_2(g) + {}^{16}O(s) + {}^{18}O(s) \quad (6)$$

We compared the behavior of parent NaX zeolite and ceria samples to the one of C20 by TPIE. Fig. 3 displays the evolution of the number of atoms exchanged (Ne) with the temperature. The curves corresponding to the NaX sample show that the zeolite oxygens are not easily exchangeable since Ne remains null below 550 °C. At 600 °C only 0.293×10^{21} atoms are exchanged, which represents less than 1.5% of the total number of oxygen atoms of the sample. It was already reported in the literature that the oxygen atoms from the zeolite skeleton were only exchanged for temperatures above 600 °C [51,52]. The number of exchanged atoms over pure ceria could be predicted: if we convert the Ne value from oxygen atom per gram of ceria (Fig. 3) to oxygen atoms per nm^2, we obtained around 50 exchanged atoms per nm^2 at 600 °C. This value matches with results reported previously and corresponds to the exchange of the surface plus two layers of the ceria bulk [53]. Surprisingly, the Ne value obtained in the case of the hybrid sample, 6.6×10^{21} atoms per gram, was largely superior to the expected Ne considering an addition of the numbers of atoms exchanged in both ceria and zeolite solids. Indeed, the contribution of each solid should give a number of atoms exchanged close to 5×10^{24} atoms per gram. Moreover looking at the evolution of the curve for hybrid sample in Fig. 3, one can speculate that the Ne value could again increase (letting the sample longer time at 600 °C) contrary to the case of ceria sample for which the equilibrium between the number of ^{18}O atoms in gas phase and in the solid was reached.

The particular behavior of the C20 hybrid sample has been confirmed by ISIE experiments carried out at 450 °C and 550 °C. We reported in Fig. 4 the evolution of the Ne values versus time for pure ceria and for C20 at the two temperatures. After 100 min, ceria exchanged 3.2×10^{21} atoms of oxygen per gram of ceria at 450 °C and 550 °C while C20 exchanges more than 4×10^{21} atoms at 450 °C and 6.7×10^{21} atoms at 550 °C (Fig. 4). It is worth noting that at these temperatures, zeolite is not able to exchange oxygen (Fig. 3).

Two hypotheses are possible to explain the greater exchange observed over the hybrid sample:

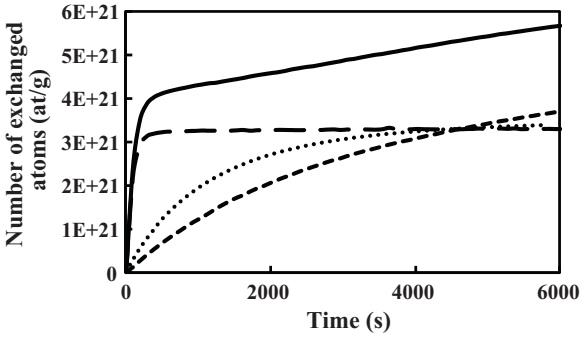

Fig. 4. Determination of the total quantity of oxygen atoms exchanged by isothermal isotopic exchange over ceria (·····) and C20 (- - -) at 450 °C and over ceria (– – –) and C20 (—) at 550 °C.

(i) The zeolite matrix improves the oxygen mobility of the ceria lattice;
(ii) The presence of ceria in the environment of the NaX exalts the mobility of the oxygen skeleton.

The first hypothesis (i) could be realistic either if the ceria crystallites were smaller in the case of the hybrid sample or if zeolite matrix provokes a confinement effect that favors the mobility of bulk oxygen atoms. On one hand, smaller crystallites lead to an increasing of the ratio between surface and bulk oxygen atoms and then more atoms might be exchanged at the same temperature. XRD patterns permitted us to exclude this possibility since the entire samples exhibit a similar size of ceria crystallites around 13 nm. On the other hand, the microporosity of the zeolite is not accessible for the ceria clusters eliminating the argument of a confinement effect. The later (ii) hypothesis seems more credible to us. We suggest that two types of exchange occur progressively on the hybrid sample: a rapid exchange of the oxygen of the ceria surface and sub-surface (in particular at high temperature) and a slower exchange of the oxygen atoms from the zeolite lattice. The rate of the second type of exchange would be increased by the presence of cerium oxide. Fig. 5 shows that the evolution during the TPIE experiment of the ratio between the partial pressures of $^{16}O_2$ and $^{16}O^{18}O$ (P_{32}/P_{34}) in the gas phase supports the idea of two successive mechanisms in the case of C20 solid. At low temperatures, both solids exhibited the same P_{32}/P_{34} ratio below 1 whereas for higher temperatures, the hybrid system displayed a specific behavior with a ratio that became superior to 1. The ratio inferior to 1 indicates that the isotopic exchange follows a simple heteroexchange as expected for ceria [53] while a ratio above 1 characterizes a multiple exchange. Chang et al. demonstrated that into ZSM-5 zeolites, the introduction of a transition metal cation increased significantly the rate of oxygen exchange via a multiple exchange [51].

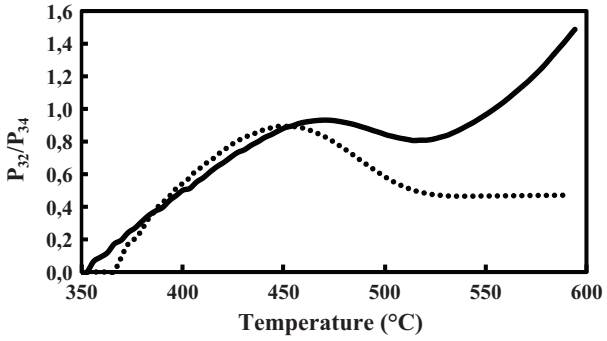

Fig. 5. Partial pressures ratio determined by isotopic exchange for C20 (—) and ceria (·····).

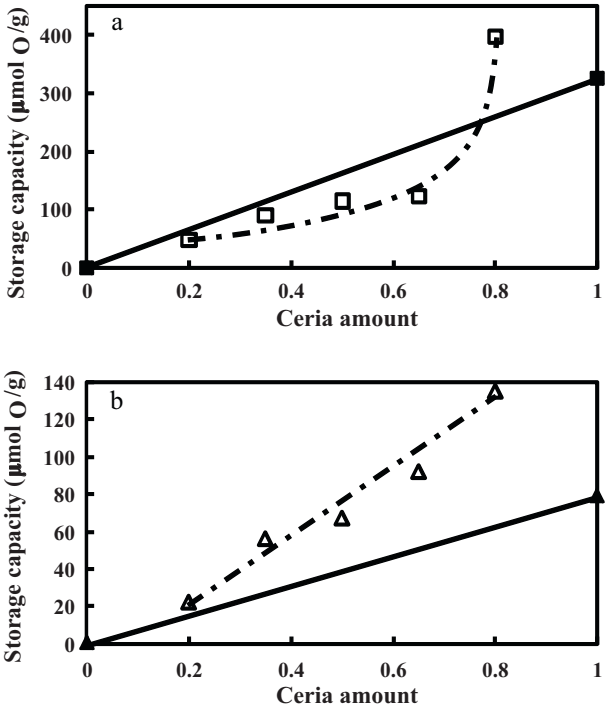

Fig. 6. Interpolated values (■) and experimental results (□) for oxygen storage complete capacity (OSCC) (a) and interpolated values (▲) and experimental results (△) for oxygen storage capacity in dynamic conditions (OSC) (b).

Although, in our case the metal incorporation is done neither by cation exchange nor by isomorphic substitution, it is possible to consider that a similar interaction occurs and that ceria addition enhances the mobility of zeolite lattice oxygen.

According to our results in oxygen storage complete capacity (static conditions), low ceria amounts seem to lower the oxygen storage capacity in comparison with the one calculated by interpolation between pure zeolite and ceria (Fig. 6a). A synergy effect given by the faujasite appears only from a ceria amount around 80% for which observed storage capacity is higher than the interpolated one. However, the storage capacity in dynamic conditions is greatly enhanced by faujasite presence whatever the ceria amount and the synergy effect gradually increases up to 80% ceria (Fig. 6b). It should be noted that results related to the oxygen storage capacity in dynamic conditions are more significant in a catalytic oxidation point of view since VOCs flow is always mixed with air and consequently with oxygen.

3.3. Catalytic oxidation

Catalytic oxidation of isopropanol was performed on each compound. Isopropanol is quickly and easily transformed into carbon dioxide and two intermediate products, which are acetone and propene. After 5 h of reaction, the conversion into carbon dioxide reaches a plateau, which is frequently already obtained since the beginning of the tests. The carbon balance was checked and was always found to be higher than 95%. According to the precision of gas chromatography analysis, such a value is quite acceptable and no undetected by-products are thus formed. Moreover, catalysts are not deactivated after 5 h of reaction and coke analysis shows a quite low amount of coke deposited since carbon percentage is always below 2 wt%.

According to our results, in most of the cases and by comparison with the performances of pure zeolite, an increasing amount of ceria clearly lowers the lightoff temperature but without however surpassing ceria performances (Fig. 7). HT35 and more HT20 make

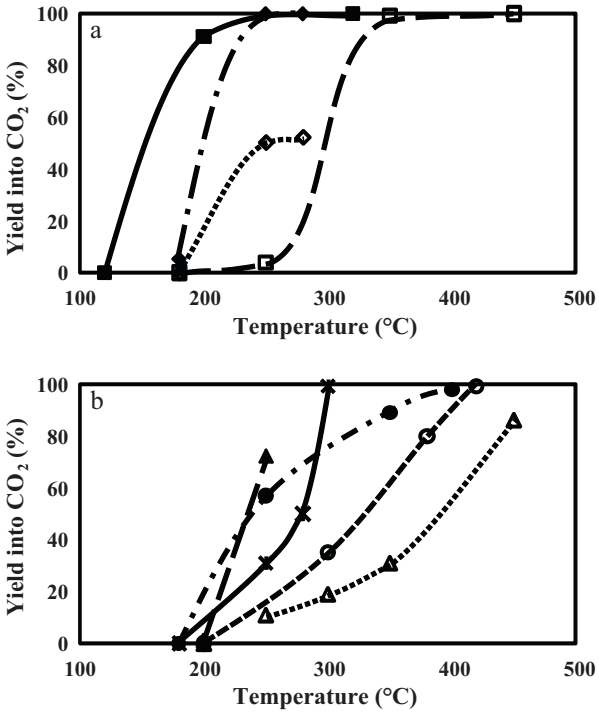

Fig. 7. Light-off curves of carbon dioxide over pure and hybrid catalysts: CeO_2 (■), HT50 (♦), M50 (◊) and NaX (□) in (a); HT80 (▲), HT65 (●), HT35 (○), HT20 (△) and C20 (*) in (b).

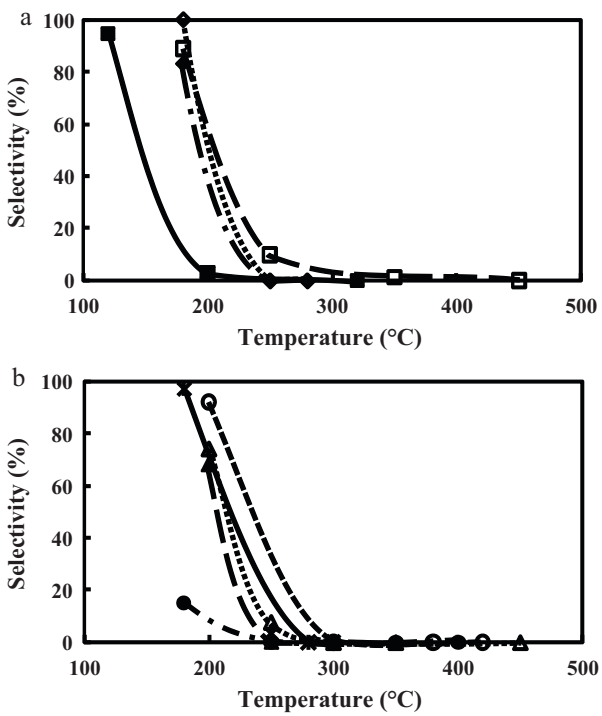

Fig. 8. Selectivity into acetone versus temperature over: CeO_2 (■), HT50 (♦), M50 (◊) and NaX (□) in (a); HT80 (▲), HT65 (●), HT35 (○), HT20 (△) and C20 (*) in (b).

exception with a conversion into carbon dioxide less important than the one of pure faujasite from 300 °C.

Making comparison between C20 and HT20, for which the main difference is the pelletizing and the sieving over HT20, it seems that this step before calcination is not appropriate for catalytic experiments since C20 exhibits better conversions into carbon dioxide than HT20 (Fig. 7b). However, calcination seems to enhance the efficiency of the catalysts since HT50 presents better results than M50 (Fig. 7a).

Only HT50 comes closer to ceria without nevertheless reaching the same efficiency. However, this catalytic formula seems to present a synergy effect. Indeed, T_{50}, temperature needed to reach 50% conversion into carbon dioxide, is equal to 150 °C for ceria and 300 °C for NaX. T_{50}, calculated with the weighted sum of each pure compound mass, would be equal to 225 °C for HT50. Experimentally, this temperature falls down to 190 °C (Table 2). The same effect could be amazingly seen at 225 °C on the carbon dioxide yield: it is equal to 95% for ceria, 3% for NaX and would be 49% for HT50 with the previous calculation method. This conversion is actually largely higher and reaches 92% (Table 2). A specific synergy effect seems then to occur on that particular catalyst.

This supposed synergy effect was checked by comparison with another catalyst (CeO_2/SiO_2) to evaluate possible effect of ceria redispersion on a support and to ensure a comparable catalytic bed height. This hybrid was prepared by mixing ceria and a high specific surface area (202 m^2/g) silica in equal weight proportion. Silica is inactive for the oxidation of isopropanol and catalytic tests with this mixture permit to evaluate the real contribution of faujasite. At 250 °C (temperature at which NaX is quite inactive in CO_2 formation) and for the same amount of ceria, i.e. 70 mg, HT50 is more efficient than CeO_2/SiO_2, with a total conversion into carbon dioxide at 250 °C against 280 °C for CeO_2/SiO_2. Comparing the T_{50}, the conclusion is similar with a T_{50} at 190 °C for HT50 and 225 °C for CeO_2/SiO_2 (Table 2). It should be noted that 225 °C is exactly the expected temperature according to the weighted mass calculation described previously. Such a result demonstrates that supporting ceria is not responsible of the observed synergetic effect and that specifically mixing ceria and basic faujasite can allow a great enhancement of the catalytic performances of the zeolite.

Unfortunately, such a synergy effect is only observed on HT50. Indeed, for most of the catalyst mixtures, CO_2 yields or lightoff temperatures do not follow a continuous and logical trend according to their ceria content (Fig. 7 and Table 2). Moreover, the shapes of the lightoff curves are quite different, some of them are very sharp

Table 2
Comparison of T_{50} and of CO_2 yield at 225 °C.

Catalysts	Calculated T_{50} (°C)	Experimental T_{50} (°C)	Calculated CO_2 yield (%)	Experimental CO_2 yield (%)
CeO_2		150		95
HT80	180	225	77	72
HT65	203	240	63	42
HT50	225	190	49	92
M50	225	250	49	41
HT35	248	330	35	10
C20	270	280	22	18
HT20	270	400	21	<10
NaX		300		3
CeO_2/SiO_2	225	225	50	50

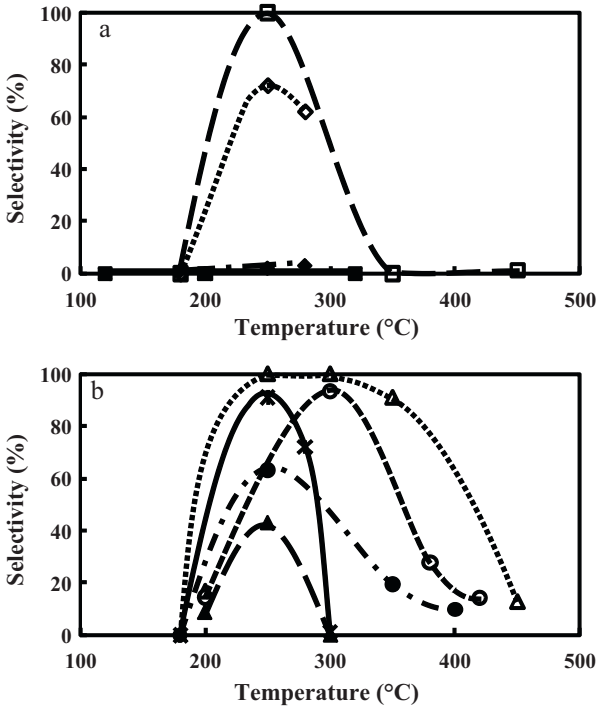

Fig. 9. Selectivity into propene versus temperature over: CeO_2 (■), HT50 (♦), M50 (◊) and NaX (□) in (a); HT80 (▲), HT65 (●), HT35 (○), HT20 (△) and C20 (*) in (b).

like the one of HT80 and the others show a very slow increase with temperature like HT35 or HT20 (Fig. 7b). These dispersed results could be explained by the numerous factors, which could interfere, like porosity, acido-basicity, ceria amount, oxygen mobility and/or storage.

Figs. 8 and 9 show the selectivity of the two main secondary products, acetone (Fig. 8) and propene (Fig. 9). The formation of acetone is easier than the formation of propene since it requires a lower working temperature. On NaX, only propene is formed while on hybrid catalysts, propene and acetone are obtained. However, HT50 presents a similar behavior than pure ceria, with propene as only secondary product. Ceria and faujasite are two basic compounds with different basic phases, which could explain the various observed selectivities.

At this stage, the explanation of the different catalysts behavior is quite difficult and needs further studies to be clarified.

4. Conclusions

Catalytic performances depend on several factors and oxygen storage capacity and oxygen mobility are often presented as key factor for catalytic oxidation. In this study, the mixing of ceria and NaX zeolite led to great increases in terms of oxygen storage and mobility. It was proposed that interaction between ceria and zeolite led to an increased mobility of the zeolite oxygen atoms.

However, this study showed by comparison of the catalytic results with the oxygen storage and exchange properties that such capabilities are not sufficient to explain the catalysts behavior during isopropanol catalytic combustion. Indeed, the catalytic performances are not correlated to the oxygen mobility results and do not follow a continuous and logical trend with ceria amount. Moreover, the different treatments carried out such as pelletizing or calcination seem to alter significantly the textural and catalytic behavior of the samples. Nevertheless, further studies focused on additional characterizations, textural properties or optimization of ceria amounts would lead to promising hybrid oxidation catalysts.

Acknowledgment

I. Maupin gratefully acknowledges the Région Poitou-Charentes for her Ph.D. grant.

References

[1] P. Le Cloirec (Ed.), Les composés organiques volatils (COV) dans l'environnement, Technique et Documentation, Paris, 1998, Chap. 1.
[2] E.C. Moretti, Chem. Eng. Prog. 98 (2002) 30.
[3] T. García, B. Solsona, S.H. Taylor, Appl. Catal. B 66 (2006) 92.
[4] D. Haffad, A. Chambellan, J.C. Lavalley, J. Mol. Catal. A 168 (2001) 153.
[5] D. Kulkarni, I.E. Wachs, Appl. Catal. A 237 (2002) 121.
[6] Y. Fukuda, H. Hattori, K. Tanabe, Bull. Chem. Soc. Jpn. 51 (1978) 3150.
[7] M.A. Aramendía, V. Borau, C. Jiménez, J.M. Marinas, A. Porras, F.J. Urbano, J. Catal. 161 (1996) 829.
[8] M. Baldi, E. Finocchio, F. Milella, G. Busca, Appl. Catal. B 16 (1998) 43.
[9] P. Papaefthimiou, T. Ioannides, X.E. Verykios, Appl. Catal. B 13 (1997) 175.
[10] D.M. Papenmeier, J.A. Rossin, Ind. Eng. Chem. Res. 33 (1994) 3094.
[11] M. Lyubovsky, L. Pfefferle, Catal. Today 47 (1999) 29.
[12] J.A. Rossin, M.M. Farris, Ind. Eng. Chem. Res. 32 (1993) 32.
[13] M. Skoglundh, L.O. Löwendahl, J.E. Ottersted, Appl. Catal. 77 (1991) 9.
[14] M.C. Álvarez-Galván, V.A. de la Peña O'Shea, J.L.G. Fierro, P.L. Arias, Catal. Commun. 4 (2003) 223.
[15] M.C. Álvarez-Galván, B. Pawelec, V.A. de la Peña O'Shea, J.L.G. Fierro, P.L. Arias, Appl. Catal. B 51 (2004) 83.
[16] R.W. van den Brink, P. Mulder, R. Louw, Catal. Today 54 (1999) 101.
[17] R.W. van den Brink, R. Louw, P. Mulder, Appl. Catal. B 25 (2000) 229.
[18] E.M. Cordi, J.L. Falconer, J. Catal. 162 (1996) 104.
[19] E.M. Cordi, P.J. O'Neill, J.L. Falconer, Appl. Catal. B 14 (1997) 23.
[20] S. Ordóñez, L. Bello, H. Sastre, R. Rosal, F.V. Díez, Appl. Catal. B 38 (2002) 139.
[21] Q. Dai, X. Wang, G. Lu, Catal. Commun. 8 (2007) 1645.
[22] S. Scirè, S. Minicò, C. Crisafulli, C. Satriano, A. Pistone, Appl. Catal. B 40 (2003) 43.
[23] W. Xingyi, K. Qian, L. Dao, Appl. Catal. B 86 (2009) 166.
[24] T. Atoguchi, T. Kanougi, T. Yamamoto, S. Yao, J. Mol. Catal. A 220 (2004) 183.
[25] J.D. Lee, N.-K. Park, S.O. Ryu, K. Kim, T.J. Lee, Appl. Catal. A 275 (2004) 79.
[26] M. Guisnet, P. Dégé, P. Magnoux, Appl. Catal. B 26 (1999) 1.
[27] S.-E. Park, J.H. Lunsford, Inorg. Chem. 26 (1987) 1993.
[28] P. Dégé, L. Pinard, P. Magnoux, M. Guisnet, Appl. Catal. B 27 (2000) 17.
[29] E. Díaz, S. Ordóñez, A. Vega, J. Coca, Appl. Catal. B 56 (2005) 313.
[30] E. Díaz, S. Ordóñez, A. Vega, J. Coca, Micropor. Mesopor. Mater. 83 (2005) 292.
[31] A.P. Antunes, M.F. Ribeiro, J.M. Silva, F.R. Ribeiro, P. Magnoux, M. Guisnet, Appl. Catal. B 33 (2001) 149.
[32] L. Pinard, J. Mijoin, P. Ayrault, C. Canaff, P. Magnoux, Appl. Catal. B 51 (2004) 1.
[33] J. Tsou, L. Pinard, P. Magnoux, J.L. Figueiredo, M. Guisnet, Appl. Catal. B 46 (2003) 371.
[34] J. Tsou, P. Magnoux, M. Guisnet, J.J.M. Órfão, J.L. Figueiredo, Catal. Commun. 4 (2003) 651.
[35] J. Tsou, P. Magnoux, M. Guisnet, J.M. Órfão, J.L. Figueiredo, Appl. Catal. B 57 (2005) 117.
[36] R. Beauchet, P. Magnoux, J. Mijoin, Catal. Today 124 (2007) 118.
[37] L. Pinard, Ph.D. Thesis, University of Poitiers, 2002.
[38] J. Tsou, P. Magnoux, M. Guisnet, J.J.M. Órfão, J.L. Figueiredo, Appl. Catal. B 51 (2004) 129.
[39] L. Pinard, J. Mijoin, P. Magnoux, M. Guisnet, J. Catal. 215 (2003) 234.
[40] L. Pinard, P. Magnoux, P. Ayrault, M. Guisnet, J. Catal. 221 (2004) 662.
[41] M. Chanda, A.K. Mukherjee, Ind. Eng. Chem. Res. 26 (1987) 2430.
[42] M. Guisnet, P. Ayrault, J. Datka, Pol. J. Chem. 71 (1997) 1455.
[43] A.L. Patterson, Phys. Rev. 56 (1939) 978.
[44] D. Duprez, J. Chem. Phys. 80 (2006) 487.
[45] S. Ojala, N. Bion, S. Rijo Gomes, R.L. Keiski, D. Duprez, ChemCatChem 2 (2010) 527.
[46] D. Duprez, Isotopes in Heterogeneous Catalysis, Imperial College Press, London, 2006, Chap. 6.
[47] D. Martin, Ph.D. Thesis, University of Poitiers, 2007.
[48] D. Duprez, Catal. Today 112 (2006) 17.
[49] D. Duprez, Spillover and Migration of Surface Species on Catalysis, vol. 112, 1997, p. 13.
[50] C. Descorme, D. Duprez, Appl. Catal. A 202 (2000) 231.
[51] Y.-F. Chang, G.A. Somorjai, H. Heinemann, J. Catal. 154 (1995) 24.
[52] J. Nováková, L. Brabec, J. Catal. 166 (1997) 186.
[53] Y. Madier, C. Descorme, A.M. Le Govic, D. Duprez, J. Phys. Chem. B 103 (1999) 10999.